

See discussions, stats, and author profiles for this publication at: <https://www.researchgate.net/publication/41531064>

Human Cardiac Troponin I: A Langmuir Monolayer Study

ARTICLE *in* LANGMUIR · MARCH 2010

Impact Factor: 4.46 · DOI: 10.1021/la903033x · Source: PubMed

CITATIONS

12

READS

67

6 AUTHORS, INCLUDING:



Jhony Orbulescu

MP Biomedicals

52 PUBLICATIONS 979 CITATIONS

[SEE PROFILE](#)



Sanja Trajkovic

University of Kentucky

13 PUBLICATIONS 135 CITATIONS

[SEE PROFILE](#)



Roger M Leblanc

University of Miami

165 PUBLICATIONS 3,732 CITATIONS

[SEE PROFILE](#)

Human Cardiac Troponin I: A Langmuir Monolayer Study

Jhony Orbulescu,[†] Miodrag Micic,^{‡,§} Mark Ensor,^{||} Sanja Trajkovic,^{||} Sylvia Daunert,^{||} and Roger M. Leblanc*,[†]

[†]University of Miami, Department of Chemistry, 1301 Memorial Drive, Coral Gables, Florida 33146,

[‡]MP Biomedicals LLC, 3 Hutton Center, Santa Ana, California 92707, [§]Department of Mechanical and Aerospace Engineering, University of California, Irvine, 4200 Engineering Gateway Building, Irvine, California 92697-3975, and ^{||}Department of Chemistry, University of Kentucky, 125 Chemistry-Physics Building, Lexington, Kentucky 40506-0055

Received August 14, 2009. Revised Manuscript Received September 25, 2009

Human cardiac troponin I (cTnI) is the preferred biomarker in the assessment of myocardial infarction. It is known to interact with troponin C and T to form a trimeric complex. Whereas small amounts are found in the cytoplasm, most of cTnI is in the form of a complex with actin located in myofilaments. To understand these interactions of cTnI better, we first investigated the surface chemistry of cTnI as a Langmuir monolayer spread at the air–water interface. We investigated the optimal conditions for obtaining a stable Langmuir monolayer in terms of changing the ionic strength of the subphase using different concentrations of potassium chloride. Monolayer stability was investigated by compressing the cTnI monolayer to a specific surface pressure and keeping the surface pressure constant while measuring the decrease in the molecular area as a function of time. Aggregation and/or domain formation was investigated by using compression–decompression cycles, *in situ* UV–vis spectroscopy, Brewster angle microscopy (BAM), and epifluorescence microscopy. To ensure that the secondary structure is maintained, we used infrared reflection–absorption spectroscopy (IRRAS) directly at the air–subphase interface. It was found that cTnI forms a very stable monolayer (after more than 5000 s) that does not aggregate at the air–subphase interface. The cTnI molecules maintain their secondary structure and, on the basis of the low reflectivity observed using BAM measurements and the low reflection–absorption intensities measured with IRRAS spectroscopy, lie flat on the subphase with the α -helices parallel to the air–subphase interface.

Introduction

One of the “holy grails” of modern diagnostics is the search for an early biomarker capable of predicting and confirming a heart attack (i.e., a myocardial infarction, MI). Since the redefinition of the diagnostic criteria of myocardial infarction in 2000, the cardiac troponins (cTns) have been regarded as the preferred biomarkers in the diagnosis of MI.¹ The new universal redefinition of MI strongly prefers cTn as the marker of choice in the diagnosis of MI.² The highly specific cardiac troponins also have prognostic value, and they have been given a central therapy-driving role in the management of acute coronary syndromes (ACSS).³ It is widely known that measurable cTn levels appear in the bloodstream only 3–6 h after the initiation of the MI process.⁴

It was shown previously that the detection of human cardiac troponin I (cTnI) is sufficient in the diagnosis of MI.⁵ In muscle tissue, cTnI forms a complex with two proteins, which are components of the troponin complex—troponin T and troponin C.^{6,7} Troponin I, in normal cells, is noncovalently attached to actin as part of the myofilaments. During cell damage and death

during an MI episode, cTnI is released and its concentration increases in the circulating blood plasma. By detecting its presence we can detect the onset of the MI. Whereas cTnI in normal cells functions as a surface-bound protein and in the disease state (MI) is found in solution, its surface chemistry properties have been, as of today, largely unknown.

One of the best ways to understand the interactions of surface proteins with their membrane and subphase environment is to study their air–water behavior by using the Langmuir film technique.^{8,9} This well-established technique allows us to produce a one-molecule-thick monolayer of proteins and to study its transformation on the air–water interface from the gaseous phase, through the liquid expanded phase, and finally to the liquid condensed phase where a protein monolayer usually collapses. Much useful information can be derived from measurements of the average molecular area and surface potential, such as protein packing and preliminary conformation studies by controlling the surface pressure. Further information can be obtained by performing additional spectroscopic and microscopic studies of the monolayer at different surface pressures.

Because the cTnI protein is mainly found complexed with actin in the myofilaments (with much smaller concentration in a cytoplasm),^{10,11} it is expected that its function is greatly influenced by surface interactions between hydrophobic and hydrophilic

*Corresponding author. E-mail: rml@miami.edu.

(1) Myocardial infarction redefined—a consensus document of The Joint European Society of Cardiology/American College of Cardiology Committee for the redefinition of myocardial infarction. *Eur. Heart J.* **2000**, *21*, 1502–1513.

(2) Thygesen, K.; Alpert, J. S.; White, H. D. *Eur. Heart J.* **2007**, *28*, 2525–2538.

(3) Heidenreich, P. A.; Alloggiamento, T.; Melsop, K.; McDonald, K. M.; Go, A. S.; Hlatky, M. A. *J. Am. Coll. Cardiol.* **2001**, *38*, 478–485.

(4) Lindahl, B. *Scand. Cardiovasc. J.* **2001**, *35*, 229–232.

(5) Ilva, T.; Lund, J.; Porela, P.; Mustonen, H.; Voipio-Pulkki, L.-M.; Eriksson, S.; Pettersson, K.; Tanner, P.; Pulkki, K. *Clin. Chim. Acta* **2009**, *400*, 82–85.

(6) Leavis, P.; Gergely, J. *CRC Crit. Rev. Biochem.* **1984**, *16*, 235–305.

(7) Filatov, V. L.; Katrukha, A. G.; Bulargina, T. V.; Gusev, N. B. *Biochemistry (Moscow)* **1999**, *64*, 969–985.

(8) Gaines, G. L., Jr. *Insoluble Monolayers at Liquid–Gas Interfaces*; Interscience Publishers, New York, 1966.

(9) Adamson, A. W.; Gast, A. P. *Physical Chemistry of Surfaces*; Wiley and Sons: New York, 1997.

(10) Mair, J.; Apple, F. *Crit. Rev. Clin. Lab. Sci.* **1997**, *34*, 1–66.

(11) Sumandea, M. P.; Burkart, E. M.; Kobayashi, T.; De Tombe, P. P.; Solaro, R. J. *Ann. N.Y. Acad. Sci.* **2006**, *1015*, 39–52.

areas of the complex filament and other cytoplasmic components and that during the process of muscular contraction troponin is exposed to a range of different surface pressures. This fact makes cTnI a surface protein, which leads us to investigate its interfacial properties in terms of surface chemistry and spectroscopy.

In this article, we utilize the Langmuir monolayer film technique to learn basic surface chemistry properties and to investigate the behavior of cTnI at the air–water interface at various surface pressures that correspond to different states, ranging from the gaseous to the liquid compressed phase. Another reason to study the Langmuir film properties of cTnI is to explore its stability and to set fundamental assumptions for future development of a thin-film-based competitive binding cTnI biosensor.

Materials and Methods

Recombinant cTnI Protein Expression and Purification.

The coding sequence for human cTnI was inserted into pET28a(+) (Novagen, division of EMD Biosciences/Merck KGA Darmstadt, Germany) and *E. coli* BL21 (DE3) cells, which were transformed with the plasmid for the expression of troponin. Cells were grown in 2 L of Lennox LB Broth (MP Biomedicals LLC, Santa Ana, CA) containing 30 µg/mL kanamycin at 37 °C × 250 rpm until the absorbance was 0.4 to 0.6. Isopropyl-β-D-thiogalactopyranoside (IPTG) was then added to a final concentration of 1 mM, and the culture was allowed to grow overnight. Purification of cTnI was based on the method published before¹² with some modifications. Cells were pelleted by centrifugation and resuspended in 40 mL of buffer A (25 mM triethanolamine (TEA), pH 7.5, 2 mM EDTA, 6 M urea). The cells were lysed with the FastPrep-24 system (MP Biomedicals LLC, Santa Ana, CA). The lysate was then centrifuged at 22 000g for 25 min. The supernatant was applied to a DEAE Sepharose Fast Flow (GE Healthcare, Uppsala) column (20 mm × 65 mm) equilibrated with buffer A. The flow-through fraction containing cTnI was collected and applied to a CM Sepharose (GE Healthcare, Uppsala) column (20 mm × 65 mm) equilibrated with buffer A. The protein was eluted using a salt gradient from 0 to 1 M NaCl in buffer A over 10 column volumes at a flow rate of 4.5 mL/min. Fractions containing cTnI were determined by SDS-PAGE and were pooled together. (The Supporting Information contains the SDS-PAGE and Western Blot data.) Ammonium sulfate to a 1 M final concentration was added to the pooled fractions and the protein was applied to a Butyl Sepharose (GE Healthcare, Uppsala) column (20 mm × 65 mm) equilibrated with buffer B (20 mM Tris/Cl, pH 7.5, 6 M urea, 1 M ammonium sulfate; all chemicals are from MP Biomedicals, LLC, Santa Ana, CA). The protein was eluted from the column using a gradient of 1 to 0 M ammonium sulfate in buffer B. Fractions containing cTnI were determined by SDS-PAGE and pooled together. The purity of the protein was determined by scanning Coomassie Blue stained gels and integrating the area under the peak using SigmaGel software. The protein was determined to be ≥97% pure. The molecular weight of the protein is 24 007 Da as determined from the known amino acid sequence. The protein expressed and purified per the protocol described above is commercially available from MP Biomedicals LLC (Santa Ana, CA).

Surface Chemistry. All surface chemistry measurements were performed in a clean room (Class 1000) with controlled temperature (20.0 ± 0.5 °C) and humidity ($50 \pm 1\%$). The measurements were performed on a KSV minitrough (Helsinki, Finland) with an area of 225 cm². The subphase used was ultrapure water obtained from a Millipore water-purification system (San Antonio, TX) and had a resistivity of 18.2 MΩ·cm and a surface tension of 72.6 mN/m at 20 °C. The surface pressure–area isotherms were recorded using the Wilhelmy method, which is, in our case, a

Whatmann filter paper soaked in ultrapure water. The surface potential–area isotherms were measured using a Kelvin probe (a vibrating electrode placed 1.5 mm above the surface and a second platinum disk electrode placed inside the subphase between which the potential was measured). Potassium chloride of purity 99.9% (MP Biomedicals LLC, Santa Ana, CA) was used to prepare solutions of different concentrations used as subphases with different ionic strengths.

Infrared Reflection–Absorption Spectroscopy (IRRAS).

The infrared spectra were acquired directly at the air–subphase interface using a Bruker Equinox55 FTIR instrument (Billerica, MA) equipped with the XA-511 accessory for the air–water interface. The trough used was a Kibron μtrough S (Helsinki, Finland) with an area of (5.9 cm × 21.1 cm) 124.49 cm². The measurements were performed using p-polarized light and a mercury–cadmium–telluride (MCT) liquid-nitrogen-cooled detector. The spectra were obtained by the coaddition of 1200 scans at different incident angles at a resolution of 4 cm⁻¹ and baseline correction using the polynomial option available in Bruker Optics' OPUS 5.5 software.

The secondary structure of cTnI in solution was determined using an FTIR accessory based on attenuated total reflectance (Bio-ATR II cell) purchased from Bruker Optics (Billerica, MA). The advantage of this cell is the low volume of solution required for measurements (10–20 µL). Data acquisition was performed by the coaddition of 1000 scans at a resolution of 4 cm⁻¹ without baseline correction.

Brewster Angle Microscopy (BAM). Brewster angle imaging was performed at the air–subphase interface using an IEllipto 2000 imaging ellipsometer provided by Accurion (Menlo Park, CA) with Bam2Plus Software. The standard laser of the BAM2-plus was a frequency-doubled Nd:YAG laser with a wavelength of 532 nm. The laser had a power of 50 mW in a collimated beam. The angle of incidence was set at 53°, near the Brewster angle for water at 53.12°.

UV–vis absorption was performed using an HP diode array spectrophotometer on a KSV minitrough (Helsinki, Finland) equipped with computer-controlled movable barriers and fitted with a quartz window suitable for absorption measurements at the air–water interface, with the lamp located above the Langmuir trough and the detector under the quartz window of the Langmuir trough.

Fluorescence at the air–subphase interface was measured using a Fluorolog-3 spectrofluorimeter (Horiba Scientifics) equipped with a bifurcated optical fiber for excitation and emission.

Fluorescence Labeling. To visualize the aggregation process better, a contrast agent was used, namely, fluorescein isothiocyanate (FITC). FITC is a commonly used fluorescent label that can be attached to proteins under very mild conditions by simply mixing the protein of interest, cTnI in the present case, with FITC over a few hours. The labeling occurs via chemical attachment of FITC through its isothiocyanate group that reacts with the amine group of the lysine amino acid present in cTnI. The labeling of cTnI was carried out in 50 mM borate buffer at pH 8.8. Unreacted FITC was removed by extensive dialysis against 30 mM Tris-HCl at pH 7.6.

Epifluorescence Microscopy. An epifluorescence microscope (model IX-FLA, Olympus) was used to acquire the fluorescence micrographs of the monolayer at the air–subphase interface at different constant surface pressures during compression on a Kibron minitrough (area available for spreading solution 5.9 × 19.5 cm², Kibron Inc., Helsinki, Finland). A thermoelectrically cooled Optronics Magnafire CCD camera detected the emission from the Langmuir monolayer.

Results and Discussion

Surface Chemistry. To obtain the optimal conditions for a stable Langmuir monolayer of cTnI, we first used ultrapure water

(12) Al-Hillawi, E.; Minchin, S. D.; Trayer, I. P. *Eur. J. Biochem.* 1994, 225, 1195–1201.

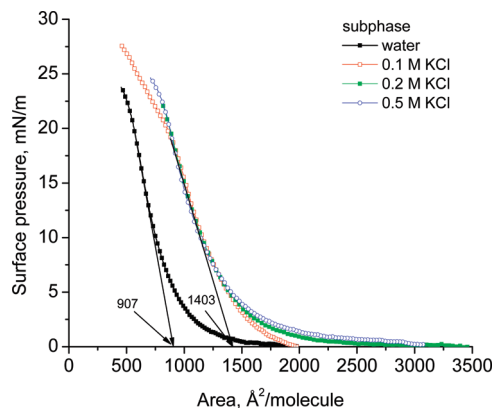


Figure 1. Surface pressure–area isotherms for 0.7 mg/mL cTnI as a function of KCl concentration in the subphase.

as a subphase. For this purpose, a solution of 0.7 mg/mL cTnI in PBS buffer (pH 7.4) was spread on the water surface. After allowing 10 min for equilibration, we compressed the monolayer at a rate of 10 cm/min.

As shown in Figure 1, the surface pressure had a lift point of around 1750 Å²/molecule on the pure water subphase. Further compression allows the acquisition of the complete surface pressure–area isotherm. The extrapolation of the linear portion of the plot gives a limiting molecular area of about 907 Å²/molecule. The monolayer collapse is not very clear but can be estimated from the change in curvature after the linear portion of the plot to be at around 22–23 mN/m.

Because the cTnI protein is water-soluble, we decided to change the ionic strength of the subphase in order to maximize the number of cTnI molecules at the air–water interface. For this purpose, we prepared a set of KCl solutions with concentrations of 0.1, 0.2, and 0.5 M.

As it can be seen from Figure 1, all three concentrations of KCl present in the subphase show a shift in the surface pressure–area isotherm toward higher molecular area compared to the pure water subphase, which means that more cTnI molecules are present at the air–water interface. Even though the surface pressure–area isotherms on KCl subphases have different lift points, their limiting molecular area was virtually the same and had a value of around 1403 Å²/molecule. The monolayer collapse can be estimated to be between 20 and 25 mN/m.

From the significant increase in the limiting molecular area, it is clear that in the case of the water subphase a large number of cTnI molecules were solubilized in the subphase because of the low ionic strength of the subphase.

Because of the fact that the three different concentrations of KCl give similar limiting molecular areas, we decided to perform the rest of the measurements using as a subphase a 0.2 M KCl solution. The choice of this concentration was solely based on the authors' decision.

The surface pressure–area isotherm was correlated with the surface potential–area isotherm by measuring both isotherms simultaneously. In Figure 2, we show the surface pressure–area and surface potential–area isotherms of cTnI spread on 0.2 M KCl. Whereas the surface pressure–area isotherm is similar to that shown in Figure 1, more information can be extracted from the surface potential measurements. It is well known that surface pressure measures mainly the interactions between molecules in close contact (usually van der Waals interactions) whereas the surface potential measures interactions at much longer distances (i.e., dipole–dipole interactions). As expected, the surface potential–area isotherm shows an increase in the surface potential as

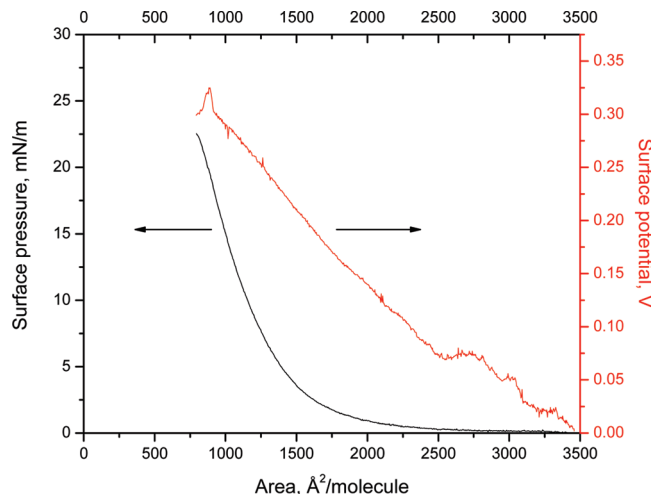


Figure 2. Surface pressure–area and surface potential–area isotherms for 0.7 mg/L cTnI spread on the 0.2 M KCl subphase.

soon as the compression of the monolayer is started. This can be explained by the charges present on the cTnI protein. When the surface pressure is still nil, we can see an increase in the surface potential. The small “bumps” are due to cTnI molecules moving rapidly on the subphase surface under the vibrating electrode at nil or very low surface pressure. When the surface pressure starts to increase, an increase in the surface potential can be seen. This increase is smooth until the monolayer collapses. Although from the surface pressure–area isotherm the monolayer collapse cannot be readily determined, the surface potential–area isotherm is more sensitive and the collapse can be estimated to be from the abrupt change observed in the surface potential at about 20 mN/m.

The theoretical pI of 9.87 was predicted from its amino acid sequence¹³ and calculated using the “compute pI/MW” tool available on the ExPASy server.¹⁴ From the calculation, it is shown that cTnI has excess positive charges—a total of 48 positively charged residues (Arg + Lys) compared to 34 negatively charged residues (Asp + Glu). Because of this fact, the cTnI molecules should repel each other when the monolayer is compressed. If our assumption is correct, then the cTnI monolayer should not form aggregates based on the Coulombic repulsion between molecules.

Indeed, our measurements using compression–decompression cycles of the cTnI monolayer confirmed this hypothesis. Figure 3 shows that the cTnI monolayer was compressed 4-fold, up to a surface pressure of 15 mN/m, but no significant changes in the surface pressure–area isotherm were observed. The lack of hysteresis in the compression–decompression cycles is direct proof that the monolayer does not form aggregates at the air–subphase interface.

So far, we have shown that the Langmuir monolayer was more stable when cTnI was spread on the KCl subphase than when the subphase was pure water, and the reproducibility of the surface pressure–area isotherms was excellent even if different concentrations of KCl solution were used as the subphase. To investigate this effect further, we decided to compress the cTnI monolayer to a surface pressure of 15 mN/m, to keep the surface pressure constant over an extended period of time, and to follow the decrease in the molecular area.

(13) Bjellqvist, B.; Hughes, G. J.; Pasquali, C.; Paquet, N.; Ravier, F.; Sanchez, J.-C.; Frutiger, S.; Hochstrasser, D. *Electrophoresis* **1993**, *14*, 1023–1031.

(14) http://ca.expasy.org/tools/pi_tool.html.

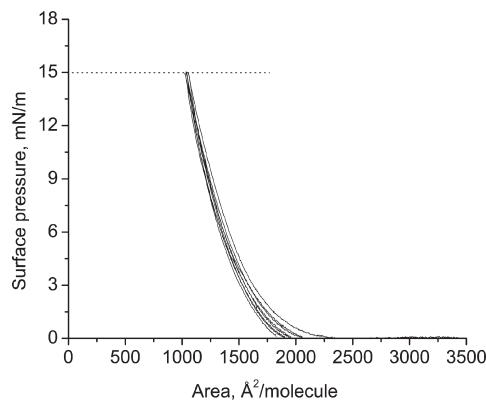


Figure 3. Compression–decompression cycles for the 0.7 mg/mL cTnI Langmuir monolayer between 0 and 15 mN/m on the 0.2 M KCl subphase.

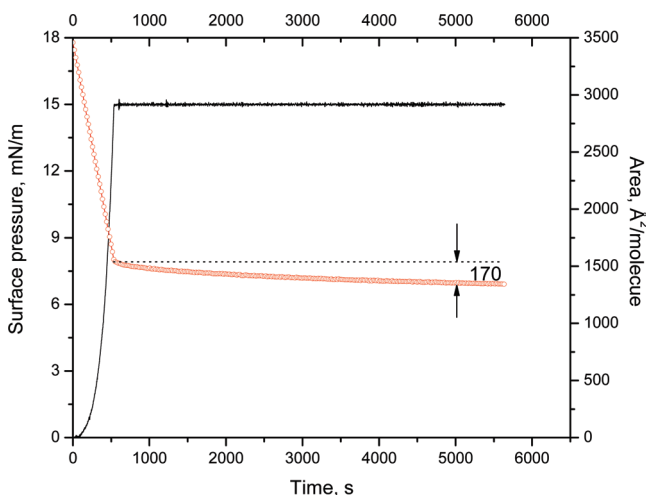


Figure 4. Stability measurement showing the decrease in area when the Langmuir monolayer of 0.7 mg/mL cTnI was compressed up to 15 mN/m and kept constant for more than 5500 s on the 0.2 M KCl subphase.

The result of this experiment is presented in Figure 4. When the cTnI Langmuir monolayer was compressed from 0 to 15 mN/m, the area decreased similarly to the surface pressure–area isotherm. The surface pressure was then kept constant after it reached a value of 15 mN/m. As can be seen from Figure 4, over a time period of 5000 s, the molecular area decreased only 170 Å²/molecule (a decrease of about 10%). The small decrease in the molecular area is proof that cTnI forms a very stable monolayer when spread on the surface of a 0.2 M KCl solution.

The results presented in Figures 3 and 4 are important for two reasons: (i) to make sure that the monolayer was not aggregating and did not solubilize in the subphase and (ii) to make sure that the monolayer did not denature during the experiment.

To confirm further the stability of the monolayer and to verify the integrity of the cTnI secondary structure (lack of denaturation), we have performed infrared reflection–absorption spectroscopy directly at the air–subphase interface.

Infrared Reflection–Absorption Spectroscopy. The infrared reflection–absorption spectra (IRRAS) are presented in Figure 5. Different spectra were collected as a function of the incident angle at a surface pressure of 20 mN/m. As shown, at angles below the Brewster angle of water (53.12°) the amide I ($1600\text{--}1700\text{ cm}^{-1}$) and amide II bands were negative ($1500\text{--}1600\text{ cm}^{-1}$) whereas at angles above the Brewster angle of water

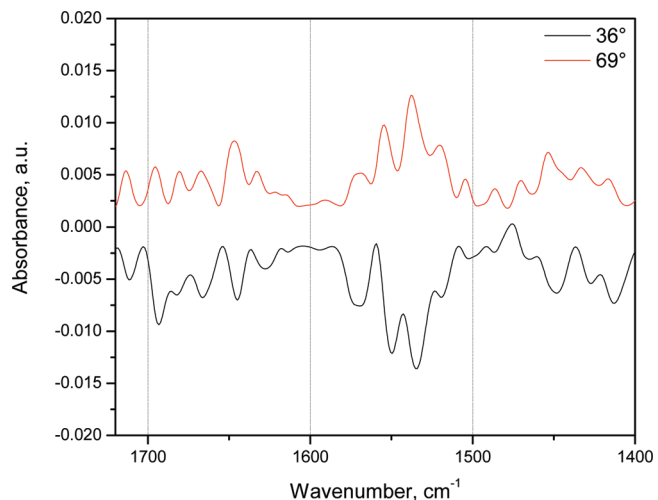


Figure 5. IRRAS spectra for 0.7 mg/mL cTnI spread at the air–subphase interface as a function of the incident angle (surface pressure fixed at 20 mN/m). Spectra were acquired using p-polarized light on the 0.2 M KCl subphase.

the bands became positive.^{15,16} This behavior is typical of molecules lying flat on the subphase (parallel to the air–subphase interface). For each spectrum, the background was taken as the 0.2 M KCl solution subphase in the absence of the monolayer.

There was no change in the secondary structure of cTnI during monolayer compression. All bands maintain their positions and were increasing in intensity under increased surface pressure. This is due to an increase in the surface density of cTnI molecules per unit area when the monolayer was compressed, which translated to a higher signal.

The spectral region shown can be divided into three main regions as follows: (i) amide I between $1700\text{ and }1600\text{ cm}^{-1}$ and (ii) amide II between $1600\text{ and }1500\text{ cm}^{-1}$ and (iii) $1500\text{ and }1400\text{ cm}^{-1}$ where the bending modes of the aliphatic C–H bands appear. Methylene (CH₂) bands are present in the side chains of the amino acids constituting cTnI.

As it can be seen from Figures 5, in the amide I region the most prominent band is centered at 1646 cm^{-1} and is assigned to the α -helix (band assignments in Table 1). There are some shoulders present around 1634 and 1621 cm^{-1} that correspond to antiparallel and parallel β -sheets and bands at 1681 and 1667 cm^{-1} typical of the β -turn and β -sheet, respectively. The secondary structure obtained at the air–subphase interface was in good agreement with the published results on the solution secondary structure of cTnI, which confirms that the main structure of cTnI is formed from four α -helices and a small number of β -sheets or turns. It must be noted that at the air–solution interface, by compression, we generated a certain number of β -sheets that are not present in solution because of side interactions between the α -helices and β -turns or coils of the cTnI molecules. A detailed description of all bands between 1700 and 1400 cm^{-1} is given in Table 1. The assignments for the amide I bands were straightforward, but amide II raised problems in band assignments because of a strong interaction with the side chains of the amino acids. The side-chain region shows an overlap of multiple different vibrational bands that are mainly due to bending and scissoring modes of C–H, CH₂, and, to a lesser extent, to C–C and C–N bending modes.

(15) Dulhy, R. A. *Appl. Spectrosc. Rev.* **2000**, *35*, 315–351.

(16) Gericke, A.; Michailov, A. V.; Huhnerfuss, H. *Vib. Spectrosc.* **1993**, *4*, 335–348.

Table 1. IR Band Assignments for Air–Subphase Interface IRRAS

| amide I (1700–1600) | | amide II (1600–1500) | side chains (1500–1400) | | |
|-----------------------------|-----------------------------------|---|-----------------------------------|--|-----------------------------------|
| assignment | band position (cm ⁻¹) | assignment | band position (cm ⁻¹) | assignment | band position (cm ⁻¹) |
| $\nu(\text{CO})$ | 1695 | Hard to assign bands properly because of the strong interaction with the side chains. | 1569 | Mainly due to $\delta(\text{CH})$ present in the side chains. Some $\nu(\text{CC})$ and $\nu(\text{CN})$ appear, which further complicates the spectrum. | 1487 |
| β -turn | 1681 | | 1555 | | 1471 |
| β -sheet | 1667 | | 1537 | | 1453 |
| α -helix | 1647 | | 1521 | | 1453 |
| antiparallel β -sheet | 1634 | | 1505 | | 1433 |
| parallel β -sheet | 1621 | | | | 1417 |

Using a Bio-ATR accessory to determine the solution ATR-FTIR spectrum of cTnI, we were also able to correlate the secondary structure of the cTnI monolayer with the solution ATR as shown in Figure 6. This result confirms, by using a different technique, that the secondary structure of cTnI was mainly due to α -helices. The main differences are that in the amide I region a major band centered at 1651 cm⁻¹ is characteristic of the α -helix and the amide II region has a single band centered at 1547 cm⁻¹. For the side-chain region, a single combination band centered at 1454 cm⁻¹ is due to the overlap in the spectrum of the different bending and scissoring modes.

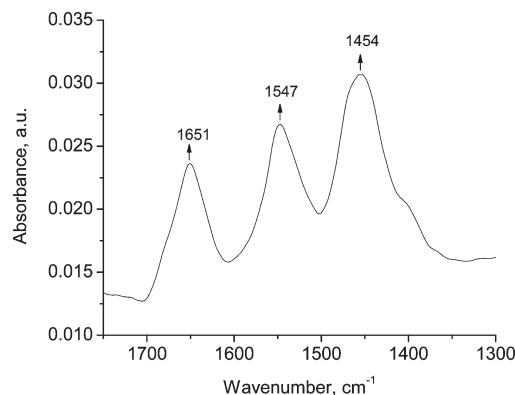


Figure 6. Bio-ATR of cTnI (0.7 mg/mL) in phosphate buffer saline (PBS) solution.

Brewster Angle Microscopy (BAM). The lack of hysteresis in Figure 3 was interpreted as a lack of aggregate formation. To investigate this finding visually, we decided to use Brewster angle microscopy. In Figure 7 are shown the micrographs obtained during compression and decompression of the cTnI Langmuir monolayer. Figure 7A shows a micrograph obtained at a surface pressure of 1 mN/m that does not show any aggregate or domain formation. This is interpreted on the basis of the homogeneity of the BAM micrograph. Further compression of the monolayer up to a surface pressure of 15 mN/m (Figure 7B) showed a very similar micrograph to that obtained in Figure 7A without any domain formation. The BAM micrograph obtained during decompression of the Langmuir monolayer to a surface pressure of 2.5 mN/m is shown in Figure 7C. These micrographs support the conclusion drawn on the basis of the data shown in Figure 3 that cTnI does not aggregate during compression–decompression cycles of the Langmuir monolayer. More information to support the lack of aggregation of the cTnI protein is given in the Supporting Information. The lack of contrast in the BAM micrographs and the very low intensities in the IRRAS spectra are indicative of a molecular orientation in which the α -helices are lying flat on the water surface, providing a low reflectivity related to the monolayer thickness and refractive index.

To confirm these findings further, we have labeled the cTnI protein with fluorescein isothiocyanate, a commonly used fluorescent label for proteins. The labeling and purification procedure is described in the Materials and Methods section.

The first observation arises from the surface pressure–area isotherm of cTnI-FITC. The new limiting molecular area is 1680 Å²/molecule for cTnI-FITC compared to 1403 Å²/molecule obtained for cTnI without the fluorescent label (as shown in Figure 8). Because the limiting molecular area is independent of the concentration used for spreading or the volume spread, we can confidently state that the increase in the limiting molecular area is due to the presence of the fluorescent label. Previously, we determined the limiting molecular area of an FITC derivative, namely, 5-octadecanoyl aminofluorescein (ODFL),¹⁷ and we have obtained a limiting molecular area for this derivative of 64 Å²/molecule. The difference in the limiting molecular areas is 277 Å²/molecule, which allows the determination of the number of FITC moieties per cTnI molecule. On the basis of this calculation, the average number of FITC groups is 4.33 for each cTnI molecule. The “classical” approach to calculating the number of FITC groups per protein is not applicable because the number of amino acids present in the structure of cTnI that are responsible for the absorption band at 280 nm is scarce. For this reason, the calculation of the ratio of A_{495}/A_{280} is practically undeterminable at the air–subphase interface, as will be shown in the section concerning UV–vis absorption at the air–subphase interface.

As shown in Figure 9, cTnI does not present any significant absorbance other than the peptide bonds present in the protein located at 206 nm. The inset shows the linear relationship between the absorbance peak at 206 nm and the surface pressure. The linear dependence is proof that during compression the surface density is increasing linearly, which in turn means that no aggregation is occurring. The first point on the inset deviates from linearity because of the fast movement of the cTnI molecules on the subphase surface whereas the deviation from linearity of the highest two points is due to the Langmuir monolayer collapse. To have proof other than the peptide absorption peak, we have used the FITC-labeled cTnI. Figure 10 shows the major absorption bands consequently assigned to FITC. The absorption bands are located at 460 and 484 nm, respectively. On the basis of the absorption spectra at the air–subphase interface, an excitation wavelength of 484 nm was selected for the fluorescence measurements of cTnI-FITC. The inset in Figure 10 shows the linearity of the absorption band at 484 nm as a function of surface pressure. On the basis of the linearity of the plot, it is clear that cTnI-FITC does not aggregate at the air–subphase interface. The fluorescence spectra obtained as a function of surface pressure at the air–subphase interface when cTnI was spread on the surface of a 0.2 M KCl solution are shown in Figure 11. The fluorescence

(17) Orbulescu, J.; Mello, S. V.; Huo, Q.; Sui, G.; Kele, P.; Leblanc, R. M. *Langmuir* 2001, 17, 1525–1528.

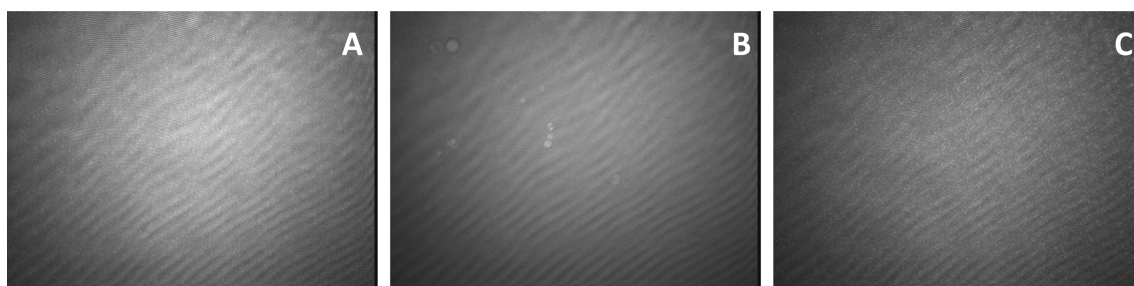


Figure 7. Brewster angle micrographs for cTnI spread on the 0.2 M KCl subphase for different surface pressures during compression, (A) 1 and (B) 15 mN/m, and decompression, (C) 2.5 mN/m (image size 200 $\mu\text{m} \times 200 \mu\text{m}$).

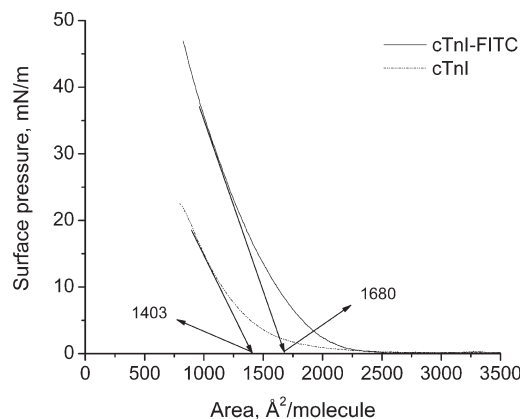


Figure 8. Surface pressure–area isotherm of 0.6 mg/mL cTnI-FITC spread on 0.2 M KCl.

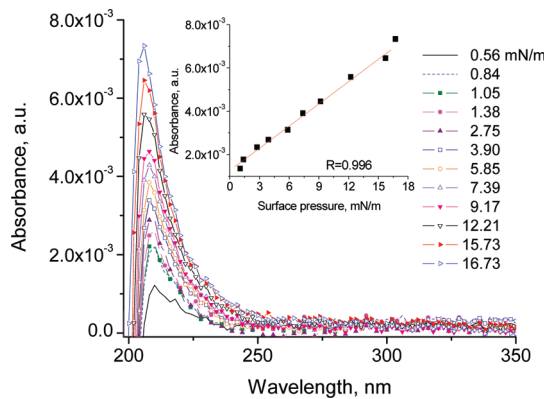


Figure 9. Absorbance at the air–subphase interface for 0.6 mg/mL cTnI spread on 0.2 M KCl as a function of surface pressure. (Inset) Absorbance maxima at 206 nm as a function of surface pressure.

maximum is located at 515 nm, which is the proper emission position taking into account the polarity of FITC. For comparison purposes, the emission spectra of octadecylamino fluorescein in solution are given in Supporting Information.

Plotting the emission maxima as a function of surface pressure reveals that the fluorescence is increasing as a function of surface pressure up to 15 mN/m (increased surface density during compression), followed by self-quenching of the FITC fluorescence (inset in Figure 11). This occurs when the cTnI-FITC intermolecular distances are reduced during compression.

Epifluorescence microscopy was performed directly at the air–subphase interface for 0.6 mg/mL cTnI-FITC on 0.2 KCl solution in order to visualize the aggregate formation directly. As shown in Figure 12, regardless of the surface pressure used no

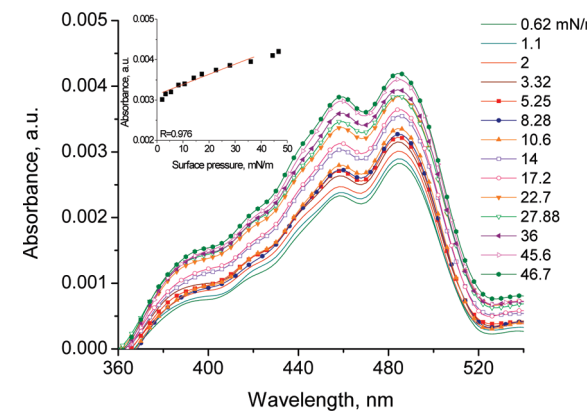


Figure 10. Absorbance at the air–subphase interface of cTnI-FITC spread on 0.2 M KCl as a function of surface pressure. (Inset) Absorbance at $\lambda_{\text{max}} = 484$ nm as a function of surface pressure.

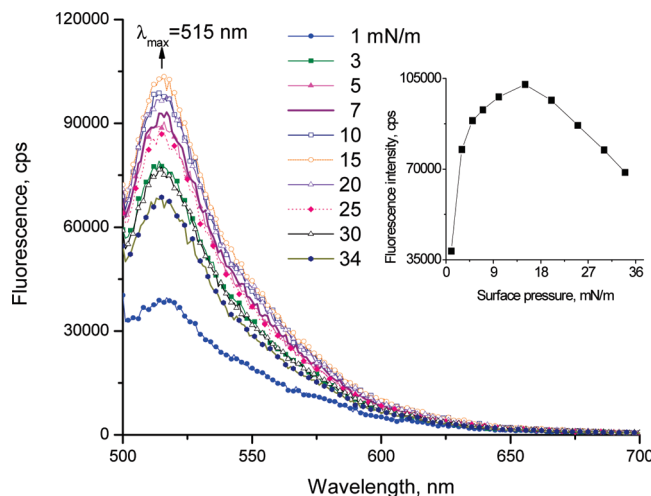


Figure 11. Fluorescence spectra of cTnI spread at the air–subphase interface on 0.2 M KCl as a function of surface pressure. (Inset) Fluorescence intensity at $\lambda_{\text{max}} = 515$ nm as a function of surface pressure.

visible aggregation can be seen. If aggregates had formed, they would have appeared as dark spots¹⁸ surrounded by green areas where no aggregation took place. Even though in Figure 11 there is self-quenching of the FITC moieties between cTnI-FITC molecules, this phenomenon is possible without the actual aggregation of the FITC-labeled protein because of possible dimer formation

(18) Kele, P.; Orbulescu, J.; Mello, S. V.; Mabrouki, M.; Leblanc, R. M. *Langmuir* 2001, 17, 7286–7290.

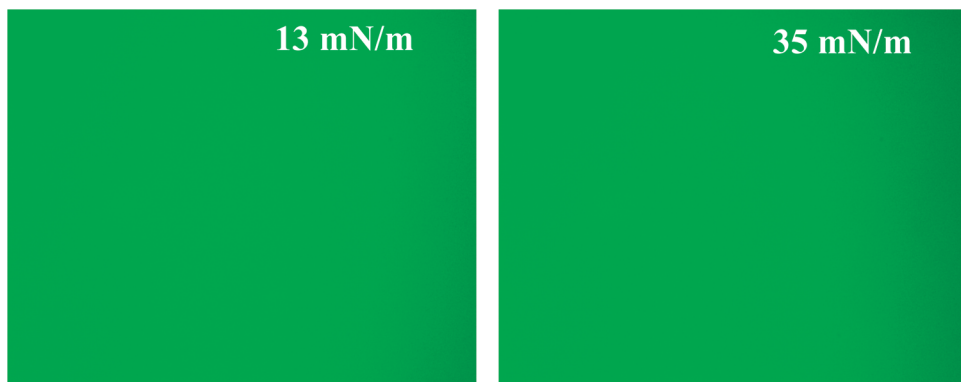


Figure 12. Epifluorescence micrographs of cTnI-FITC spread at the air–subphase interface. The micrographs were taken during compression for two surface pressures of 13 and 35 mN/m, respectively (image size, 895 $\mu\text{m} \times 713 \mu\text{m}$).

at the high surface density of cTnI-FITC (high surface pressures) that cannot be detected on the μ scale of the epifluorescence measurements.

These measurements support the results explained in the article regarding the lack of aggregation during cTnI monolayer compression.

Conclusions

It was shown that cTnI forms a very stable Langmuir monolayer if the ionic strength of the water subphase is increased by the addition of KCl. The Langmuir monolayer formed does not lead to domain or aggregate formation, and the secondary structure of cTnI is similar to that obtained in solution using Bio-ATR FTIR. On the basis of the limiting molecular area, BAM micrographs, and the infrared intensities obtained with p-polarized IRRAS, the molecular orientation is one in which the main component of the secondary structure (i.e., α -helices) lies parallel to the air–subphase interface.

Acknowledgment. R.M.L. is grateful for the financial support provided by the University of Miami, College of Arts and Sciences, under Bridge Grant Funding and the National Science Foundation under grant no. CBET-0944290. This work was supported in part by various grants from the National Institutes of Health and the National Aeronautics and Space Administration. S.D. acknowledges support from a Gill Eminent Professorship.

Supporting Information Available: Additional data are presented regarding SDS-PAGE, Western Blot, the surface pressure–area isotherm for cTnI labeled with FITC, UV–vis spectroscopy at the air–subphase interface, and epifluorescence imaging. A brief description of these methods is given along with the supporting results and discussion. This material is available free of charge via the Internet at <http://pubs.acs.org>.